COMPARISON OF CONTINUOUSLY FILTERED GPS CARRIER-PHASE TIME AND FREQUENCY TRANSFER WITH INDEPENDENT DAILY GPS CARRIER-PHASE SOLUTIONS AND WITH TWO-WAY SATELLITE TIME TRANSFER

Demetrios Matsakis, Ken Senior, and Phyllis Cook
U.S. Naval Observatory

Abstract

Several different modes of precise time transfer are currently in use or under development. These include GPS common view, two-way satellite time transfer, and GPS carrier phase. The U.S. Naval Observatory has accumulated several years of data analyzing these techniques with side-by-side comparisons over short, intermediate, and long baselines. Each technique can offer something to the mix, and we use the comparisons to discuss the strong points and weaknesses of each one.

I. INTRODUCTION

Precise time transfer can be achieved by a variety of techniques, including GPS common view (CV), GPS carrier phase (CP), and two-way satellite time transfer (TWSTT). The U.S. Naval Observatory (USNO) regularly makes use of these time-transfer techniques over both short and long baselines. This work compares the stabilities of these different techniques, with an emphasis on long-term stability. Of the GPS techniques, we will compare continuously filtered carrier-phase with independent daily carrier-phase solutions, but emphasize continuous filtering, since it appears to be more precise and at least as accurate as the other GPS techniques. Issues relevant to calibration, as distinct from long-term stability, are covered here only in the sense that whatever technique proves to be most stable in the long term would also be the most accurate if side-by-side comparisons are used to provide the relative calibrations needed for time transfer.

II. HARDWARE AND DATA ANALYSIS

Multiple GPS receivers are in operation at USNO in Washington, D.C. (USNO-DC) and its Alternate Master Clock (USNO-AMC) facility in Colorado, including single- and dual-frequency standard positioning service (SPS), precise positioning service (PPS), single-channel, and multi-channel receivers. Non-geodetic PPS and SPS estimates of UTC (USNO) minus GPS Time are reduced according to the standards set in **[1]** and procedures described in **[2]**. Ionosphere corrections are available through model or dual-frequency measurements. Individual receivers are compared by zero-baseline CV, and relative calibrations are preserved by infrequent software adjustments. CV data were reduced using broadcast orbits, as described in **[2]**.

TWSTT data reported between the USNO and other institutions form part of the data series now used operationally for the generation of Coordinated Universal Time (UTC) and International Atomic Time (TAI). TWSTT data between USNO-DC and USNO-AMC and for short baselines within USNO-DC are

obtained using different modems and satellites, and have been affected by several problems with the modems, beginning in November 1999 (approximately MJD 51500). These problems, indicative of the greater complexity of TWSTT hardware, were rectified over the subsequent few months. A significant improvement is expected when new TWSTT modems, which use carrier-phase information, are made operational [3].

Most of the CP time-transfer data used here are publicly available from the archives of the International GPS Service (IGS). Most of the CP time-transfer results used here are from in-house continuously filtered solutions using JPL's GIPSY-OASIS II package [4]. Due to computer limitations, the smoothing (backwards filtering) was limited to 10 days. Since missing data or receiver resets require reinitializing filter parameters for a given site, continuous filtering still has some discontinuities in it. In addition, some CP-based time-transfer solutions were downloaded from the CODE analysis center, which uses the Bernese software package, and from the USNO Earth Orientation Department's solutions, which are based upon GIPSY.

A summary of the CP receiver/systems designations is given in Table 1; more detailed explanations of their configurations are given below.

Table 1. Brief summary of CP receivers located at the USNO. Acronyms and other details are provided in the text. AMC2, NIM1, NIM2, and USNZ are kept in rooms whose temperature is constant to roughly 1 deg C. The receivers designated USNB and USNO are usually kept thermally stable to about 0.1 deg.

Designation	Location	Receiver Model	Owner
AMC2	USNO-AMC	TurboRogue/ACT	USNO
NIM1	USNO-DC/Bldg.78	Ashtech Y12	NIMA
NIM2	USNO-DC/Bldg. 78	Ashtech Y12	NIMA
USNB	USNO-DC/Bldg. 78	Ashtech Z12T (GeTT)	SFOM
USNO	USNO-DC/Bldg. 52	TurboRogue/ACT	USNO
USNZ	USNO-DC/Bldg. 78	Ashtech Z12T	USNO

The USNO CP data reported to the IGS are derived from two TurboRogue receivers, manufactured by Allen Osborne Associates (AOA), and their systems are designated to the IGS as USNO (located at USNO-DC) and AMC2 (located at USNO-AMC). An issue that has posed a serious problem for potential CP time users is that many first-generation timing receivers are uncalibratable. The TurboRogue and Ashtech Z12 models are subject to random timing jumps with every power reset, a problem which became more frequent for the USNO after it upgraded its TurboRogues to the ACT design (MJD 51245 for the receiver AMC2; MJD 51477 for the receiver USNO). Hereafter, the term TurboRogue will be used to designate both the pre-upgrade and post-upgrade models, and in both cases their data can often be corrected using measurements of the receiver's 1 pulse-per-second (1-pps) output against the timing reference [5,6]. Figure 1 (top) shows uncorrected time transfer between the receiver USNO and the GeTT receiver, which is described in next paragraph. Figure 1 (middle) shows how those corrections improved with the use of 1-pps data. After the upgrade for the receiver designated USNO, the corrected data become trimodal, a fact that may be related to the shape of the 1-pps output pulse, and which was not the case for a similar receiver at the USNO-AMC. Figure 1 (bottom) shows the frequency transfer inferred after accounting for the trimodal nature by applying systematic corrections to each of the three

modes, with just one correction per mode. Each mode was corrected by subtracting *ad hoc* offsets that appeared to minimize the time-transfer variations, and deleting outliers.

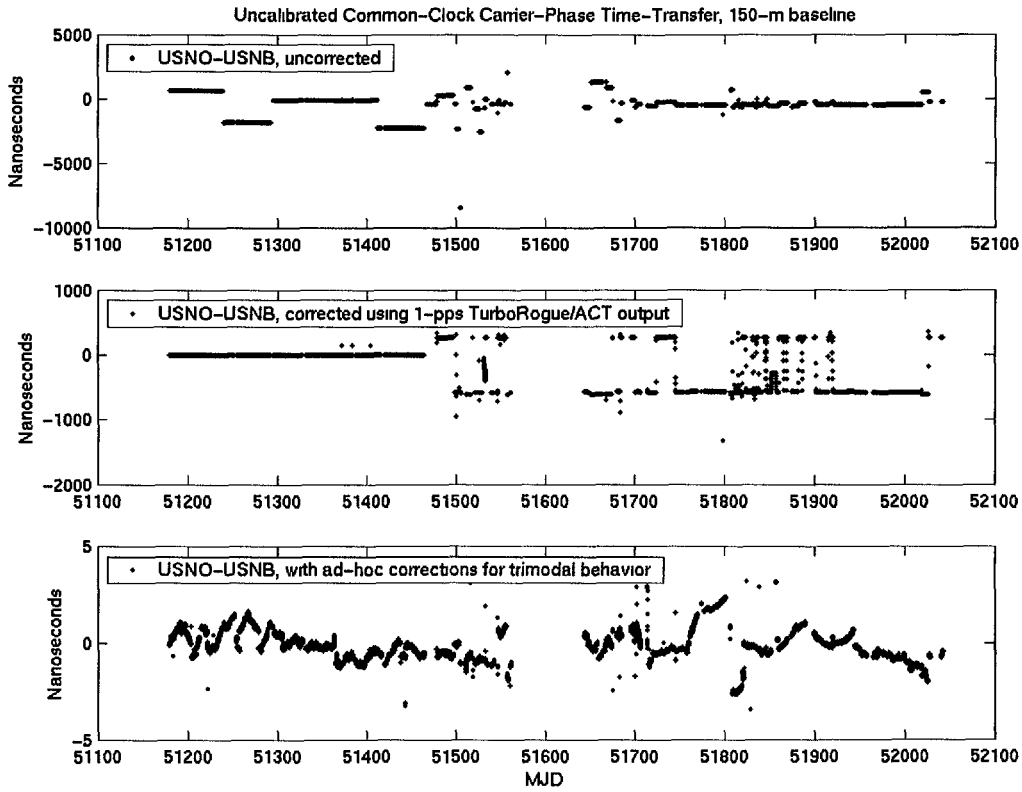

Figure 1. Corrections to carrier-phase data on the 150-m baseline between two buildings at USNO-DC. Top plot gives the raw data; the middle plot gives the data corrected using the 1-pps output as in **[5]**; and the lower part includes systematic corrections for the trimodal behavior after MJD 51490. Data were referenced to a common clock using round-trip fiber-optic measurements.

Until the spring of 2001, the USNO's CP program benefited from the loan by the Swiss Federal Office of Metrology (SFOM) of a Geodetic Time Transfer Terminal (GeTT), which was directly referenced to UTC (USNO) **[7]**. The GeTT's receiver is an Ashtech Z12T normally kept at 15 degrees C in a temperature-controlled chamber, but which began to fail on roughly MJD 51760. Its temperature was 4 deg C on MJD 51806, when it was set to 35 deg C as a test. On MJD 51820, the chamber was returned to normal operating temperature **[8]**. The gap in GeTT data from MJD 51561-51644 is due to a computer problem. The Ashtech Z12T is an Ashtech Z12 receiver modified to correct the problem of receiver calibration loss between resets; a similar fix for the TurboRogues has recently been developed **[9]**.

Also reported here are CP data from two Ashtech Y12's (designated NIM1 and NIM2), which are in the same room as the GeTT. They are located adjacent to each other, share a common antenna, and are owned and operated by the National Imagery and Mapping Agency (NIMA). Their design is similar to the Z12, and includes a phase-lock loop, which could be contributing to their instabilities reported below **[10]**.

Finally, some recent data are described that were taken using an Ashtech Z12T, designated USNZ and referenced to UTC (USNO), which was recently introduced as a contributor to the JPL real-time differential GPS network [11].

III. ZERO AND VERY-SHORT-BASELINE, COMMON-CLOCK STUDIES

At USNO, zero-baseline and short-baseline time transfer is conducted routinely between devices referenced to a common clock. Many potential error sources, such as mismodeled atmosphere, ionosphere, or orbital parameters will largely cancel on the very shortest baselines. These experiments provide a framework to identify or characterize instabilities due to factors such as multipath environments and hardware that is aging, environmentally sensitive, or simply temperamental.

Figure 2 shows all possible timing differences between the three Ashtech CP receivers located at USNO, and also the temperature of the room in which they are located. None of the receivers is completely calibrated in an absolute sense, and three "spontaneous" timing jumps in the two Ashtech Y12's designated NIM1 and NIM2 were adjusted by systematic ad-hoc bias corrections. The variations in the GeTTs timing data beginning MJD 51760 are due to the failure of and experimentation with the GeTT's temperature control circuits, as previously described. The effect of a failing Ashtech Y12 (NIM2) at MJD 51650, and its subsequent replacement, is also evident. In contrast, the response to the temperature adjustment on MJD 51324 seems to indicate that small changes in the room temperature can lead to a few nanoseconds of time-transfer variation in the Ashtech Y12's. The plots also show that these receivers can vary slowly by up to 10 nanoseconds. Our data do not rule out the possibility that the observed differences are due to cable multipath induced by the passive power splitter used to distribute the signal to NIM1 and NIM2 from their shared antenna; however, receiver-dependent temperature effects sufficient to cause the problem are reported in these Proceedings [12].

IV. SHORT (100-150 METER) BASELINE STUDIES

The USNO-DC maintains clock ensembles in two buildings. The TWSTT and CV equipment are separated by 100 meters, while the CP equipment are separated by 174 m. Time transfer is achieved by TWSTT, CV, CP, several runs of optical fiber, and comparisons with a portable cesium clock. The one-way differences from the fiber, cable, and portable clock measurements show both seasonal and long-term variations that total less than 1 nanosecond over periods of years. One-way diurnal variations of up to 100 ps are observed with an hourly measurement precision of 20-50 ps; one-way seasonal and long-term one-way variations can be of order 1 ns [13]. Consistency, and probably accuracy, are achieved at the level of several hundred picoseconds rms through round-trip corrected links using laser/LED-based fiber-optic signals, and (since MJD 51820) passive phase-stable cables. The consistency of this process is confirmed by repeated calibration through direct measurements using a portable cesium clock [M. Tran, USNO, private communication]. This consistency, based on three entirely ground-based measurement modes, suggests that the few-ns long-term variations in the difference between ground and CP or TWSTT time transfer (Figure 3) are due to the space-based techniques themselves. The variations are not consistently temperature-related, although the CP for all the USNO systems except USNZ are carried out without temperature-stabilized antennas. Although we conclude below that the code data of the antenna designated USNO has a low temperature dependency, that of the antenna associated with the GeTT could be as high as 100 ps/deg [7] and result in a few-ns variation over the 25-deg C seasonal temperature

differences. The most important information in this comparison may be how small the long-term differences are in Figures 3 and 4; a 5-ns shift over 100 days is a frequency error of only 5.8 10^{-16}.

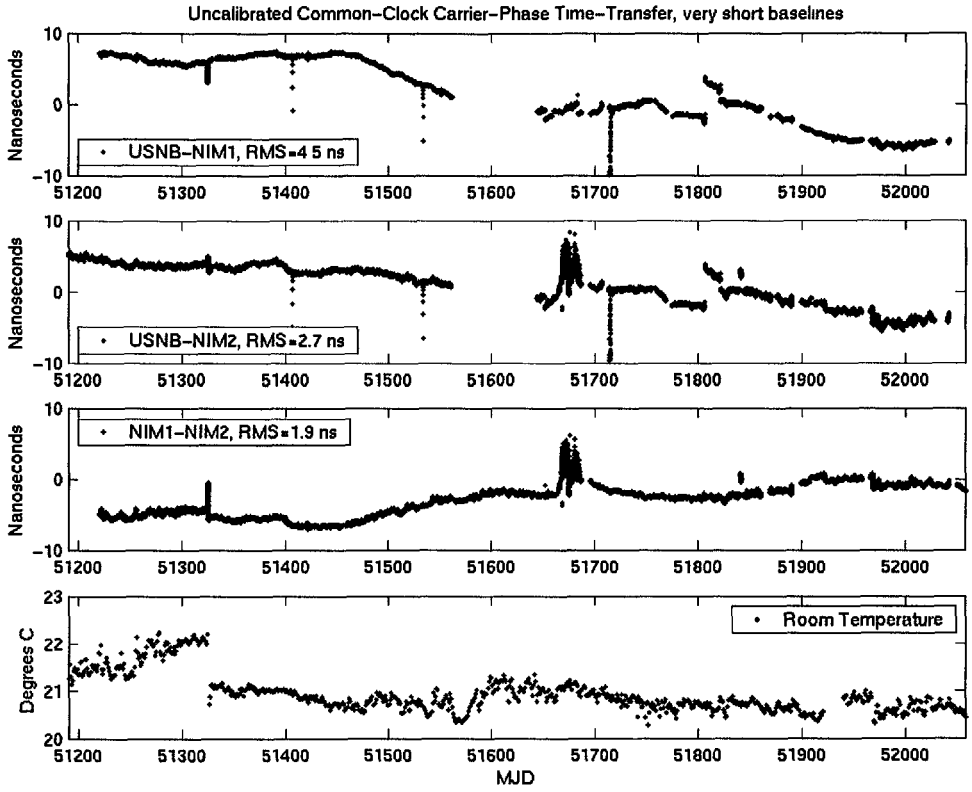

Figure 2. Timing difference between three receivers kept in the same room. The GeTT's receiver, designated USNB, is temperature-stabilized. The receivers NIM1 and NIM2 share a common antenna and signal splitter. The failure of the Ashtech Y12 beginning at MJD 51650, and its subsequent replacement are evident, as are the variations in USNB due to the failure and replacement of its temperature-stabilizing circuits, from MJD 51760 to MJD 51806. The GeTT's antenna cables were replaced by temperature-compensated cables on MJD 51714. Comparisons with the receiver USNO, in the next figure, indicate that most of the variations are probably due to the NIMA receivers. The GeTT's temperature-control circuitry generally keeps its receiver's temperature constant to about 0.1 deg C. Data from NIM1 were stepwise adjusted by *ad hoc* corrections for jumps due to system resets on MJDs 51399, 51690, 51742, 51744, 51944, and 52034. Data from NIM2 were similarly adjusted for system resets on the same days as NIM1, and also on MJD 51967. Room temperature is a daily average.

V. CONTINENTAL BASELINES

Figures 5 and 6 compare dual-frequency CV, TWSTT, and CP data between the USNO-DC and USNO-AMC. It can be seen in these figures that variations on the order of 10 ns peak-to-peak can occur over periods of 200 days, as with the short baseline, corresponding to frequency drifts of 5.7 10^{-16}. Because the USNO DC-AMC TWSTT is calibrated about every 6 months, the data provide some evidence that TWSTT is more stable on these scales. Improved monitoring, using either multiple stationary systems or

relative calibration with portable equipment transported between sites, could help sort out the long-term trends. It is also important to realize that the differences between the techniques may be due to hardware problems in the specific equipment used, and that similar time-transfer equipment made by either the same or different manufacturers could produce different results.

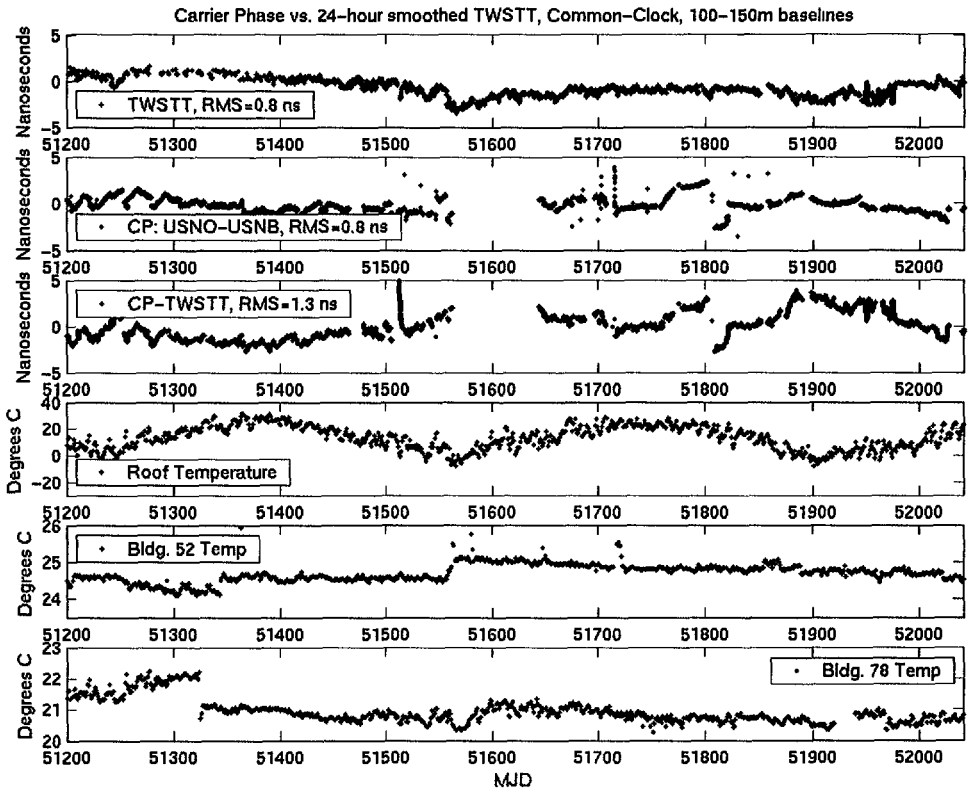

Figure 3. Comparisons of TWSTT and CP time-transfer between two buildings at USNO-DC. Calibration is achieved via round-trip corrected optical fibers and phase-stable cabling. CP data are between the systems designated USNO and USNB (GeTT). For this plot, TWSTT data are smoothed by averaging over 24 hours. TWSTT variations over MJD 51550-51580 and CP variations over MJD 51760-51821 are due to known hardware problems. The "Roof Temperature" is the daily average as measured above Bldg. 52. The "Bldg. 52 Temp" plot is the daily average temperature of the chamber housing the receiver USNO and the interface for the ground-based timing tie between the two USNO-DC buildings. The "Bldg. 78 Temp" plot is the daily average temperature of the room housing USNB and the other end of the timing link between the two buildings. Portable clock trips calibrate the ground links to a few hundred ps.

VI. DIURNALS IN TIME AND FREQUENCY TRANSFER

Diurnal variations (diurnals) are observed in almost all kinds of measurements; time and frequency measurements are no exceptions. The study of diurnals provides a crude measure of a technique's sensitivity not only to temperature variations, but also multipath and any error source that repeats with a near-24-hour period. Sites that have thermally controlled masers for their time standards typically have internal timing variations less than 100 ps/day; any observed diurnal signature equal to or larger than this

can be ascribed to the time-transfer technique. Diurnal signatures cannot, in general, be observed with CV data because daily averages are used to achieve improved signal-to-noise and mitigate multipath effects. However, diurnals are observed in almost every site for both CP and TWSTT, and their amplitudes can be as high as 1 ns. Diurnal variations tend to be larger in the summers than the winters for some sites, but not others. We suspect that those CP sites that show diurnal variations exceeding 200 ps probably have exterior cables whose delays are not temperature-compensated **[14]**, but we have not done any investigation to demonstrate that this is true. One study of the TurboRogue data for the USNO-DC vs. USNO-AMC CP links that do have temperature-compensated cables (but whose antenna electronics are exposed to the outdoor environment) showed no statistically significant correlation with site temperatures, to a limit of 2 ps/deg C **[15]**. Laboratory measurements of one commonly used antenna electronics package (the narrow-band system marketed by AOA) revealed group-delay temperature dependencies as high as 100 ps/deg C at some frequencies in the range of 1206-1595 MHz; the inferred dual-frequency temperature dependency was 40 ps/deg C near the GPS center frequencies **[6]**. More precise laboratory measurements of phase and code variations are in progress [E. Powers, USNO, private communication].

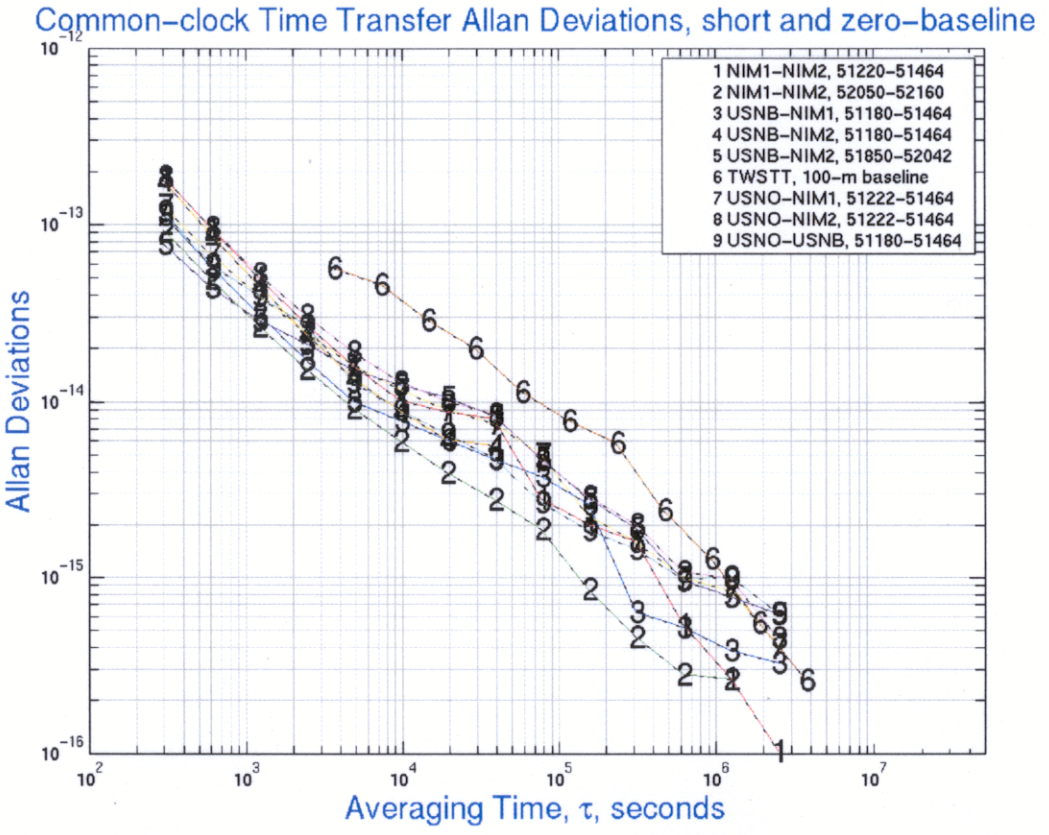

Figure 4. Allan deviation of short- and zero-baseline common-clock time-transfer data, over periods of "normal" instrumental performance. Median slope for carrier-phase Allan deviations, for tau < 10,000 sec, is observed to be -.77. For this plot, TWSTT data were taken from MJD 51024-52219 and not smoothed in any way. Common-clock reduction for the data involving TWSTT and the receiver USNO was achieved by interpolating round-trip measurements, whose underlying hourly measurements have a precision of 20-50 ps. The greater short-term precision of GPS carrier phase and equivalent long-term performance of TWSTT are evident.

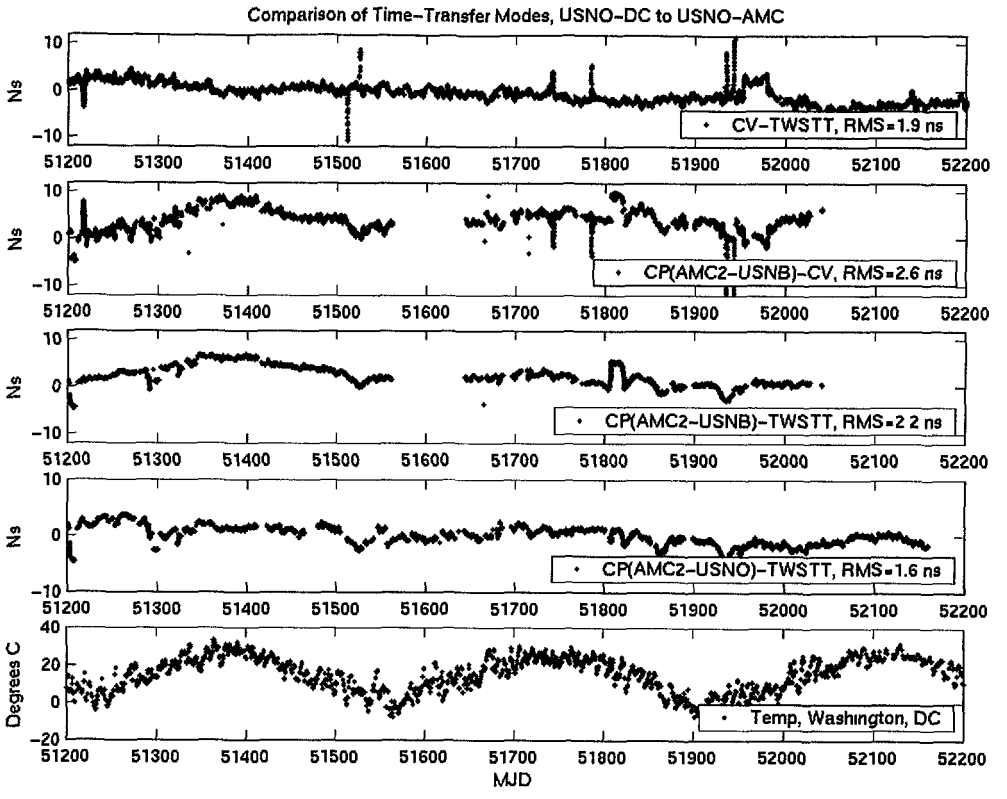

Figure 5. Time transfer between USNO-DC and USNO-AMC. For this plot, TWSTT data are averaged over 24 hours. Calibration is achieved via TWSTT, at the 1-ns level, at approximately 6-month intervals. Most of the abrupt few-ns, few-day variations are due to known equipment failure. CV data are from dual-frequency 1-pps receivers.

To investigate the diurnal signatures, a simple filter was created. Data were first filtered by subtracting from each point the average of the preceding and following 12 hours; then the filtered data were averaged in 10-day batches, after having been sorted into bins of 0.1-day duration, modulo 24 hours. If the curve of 24-hour filtered data is denoted $d(t)$, then the plotted average value, $y(t)$, can be expressed as $y(t) = \frac{1}{10}\sum_{n=1}^{n=10} < d(t,n) >$, where t is in days, n is a day-index, and $< d(t,n) >$ is an average of the filtered data $d(t,n)$ from $t = t'_n$ to $t = t'_n + \frac{1}{10}$, where $t'_n = t_{\mathrm{mod}\,10} + n + \frac{1}{10} t_{\mathrm{mod}\,1}$. It must be stressed that this filter would tend to suppress any signal whose frequency is not an integer multiple of 1 day. In all cases cited in this paper, an independent Fourier analysis has revealed no significant signal at frequencies that the filter would suppress.

As an example, Figure 7 shows how this process would work on a computer-generated signal. The process of generating a 10-day binned diurnal variation is further illustrated in Figure 8.

Figure 9, generated with the above diurnal-enhancement procedure, shows a diurnal term between USNB (the GeTT at the USNO) and the receiver designated USNO, which is variable but often near 100 ps peak-to-peak. Possibly this is entirely due to 2-5 ps/deg delay variations of the GeTT's antenna and cabling. Figure 10 shows a similar diurnal term for TWSTT in the continental baseline between USNO-DC and USNO-AMC and between short-baseline runs between two buildings at USNO-DC; the variation is seasonal on the long baseline, but not the short. Note that the diurnal temperature variations tend to be larger in the summer than the winter (1 January 2000 was MJD 51544).

Temperature variations are not the only possible cause for diurnal variations. Relative humidity, which is strongly correlated to temperature, could also be a factor. Variations could be due to carrier, code, or cable multipath **[14,16]**. Ionosphere mismodelling could contribute diurnally to single-frequency GPS observations **[17]** if the data were not averaged into one-day batches. Much of the TWSTT diurnal signature could be due to slightly different temperature coefficients in the antenna hardware for the uplink and downlink paths, but ionosphere or orbit mismodelling could also make small contributions **[18]**. If the magnitude of the diurnal fluctuations were used to compute an upper bound to the temperature dependency, then the seasonal fluctuation should be 2-3 times larger, commensurate with the seasonal temperature variations, and if so it would be dwarfed by clock instabilities, since even 3 ns in 6 months corresponds to a frequency change of $< 2\ 10^{-16}$.

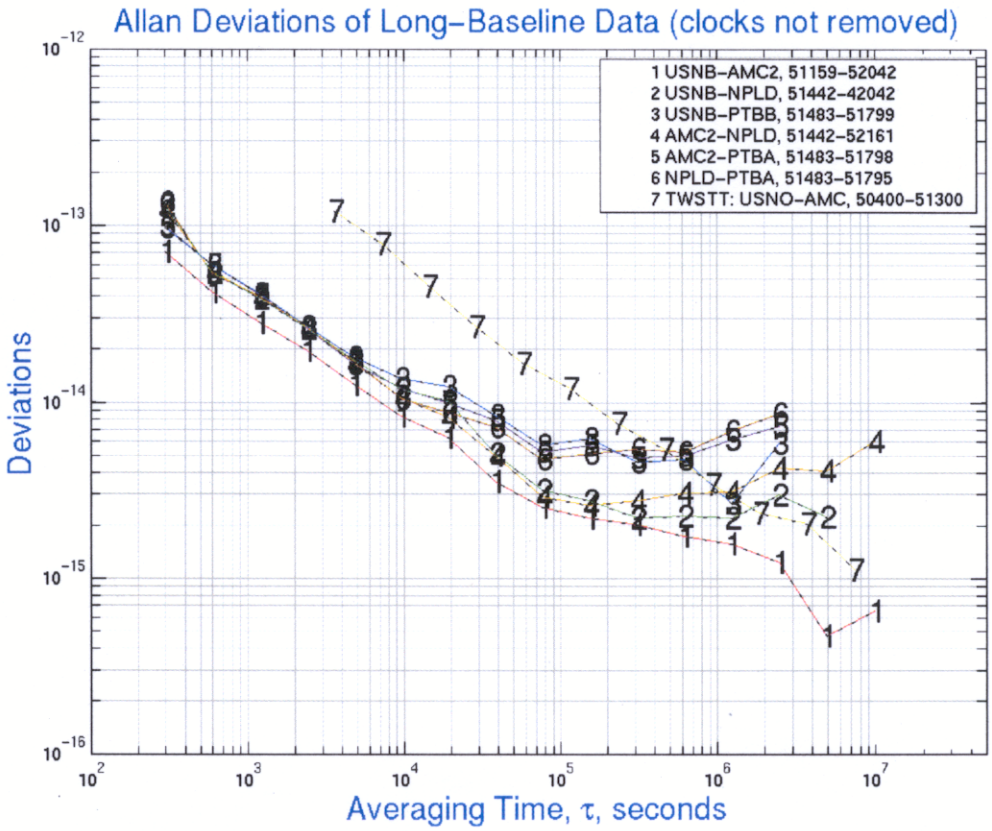

Figure 6. Allan deviations of long-baseline data. USNO DC-AMC data can be considered common clock to 1 ns rms, since the AMC master clock is steered to the USNO Master Clock via semi-annually calibrated TWSTT. No data were smoothed. NPLD and PTBB are carrier-phase GPS receivers at NPL (England) and the PTB (Germany). Median slope of carrier-phase Allan deviations for tau < 10,000 seconds is observed to be -.65.

VII. USE OF CODE RESIDUALS OF CARRIER-PHASE GPS TO DETERMINE ENVIRONMENTAL SENSITIVITY

In GPS solutions that include both code and phase data, the SNR difference of 100 leads to phase data receiving 10,000 times the weight of the corresponding code data. Since with today's technology, the integer-wavelength ambiguity between phase and code is a parameter to be solved for, phase data can only give information about frequency transfer. To achieve time transfer, one overall constant must be determined from the code. Since code data are more susceptible to multipath and environmental variations, one can use the code data residuals to study these error sources. The code residuals are the pseudorange data corrected for all effects modeled by GIPSY solutions, among them orbits, site position, earth orientation, atmosphere, ambiguities, and clock frequencies. With the exception of the ambiguities, the corrections are identical for corresponding code and phase data. The difference between the code and the phase-temperature dependencies, therefore, should appear in the difference between the code and the phase residuals. The effects of phase-temperature dependencies are absorbed in the fitted clock parameters and can be determined by observing the correlation of temperature with the subdaily time (frequency) variations. The diurnal signatures of the code residuals from several sites, produced using the filter described in Section VI, are shown in Figures 11 and 12.

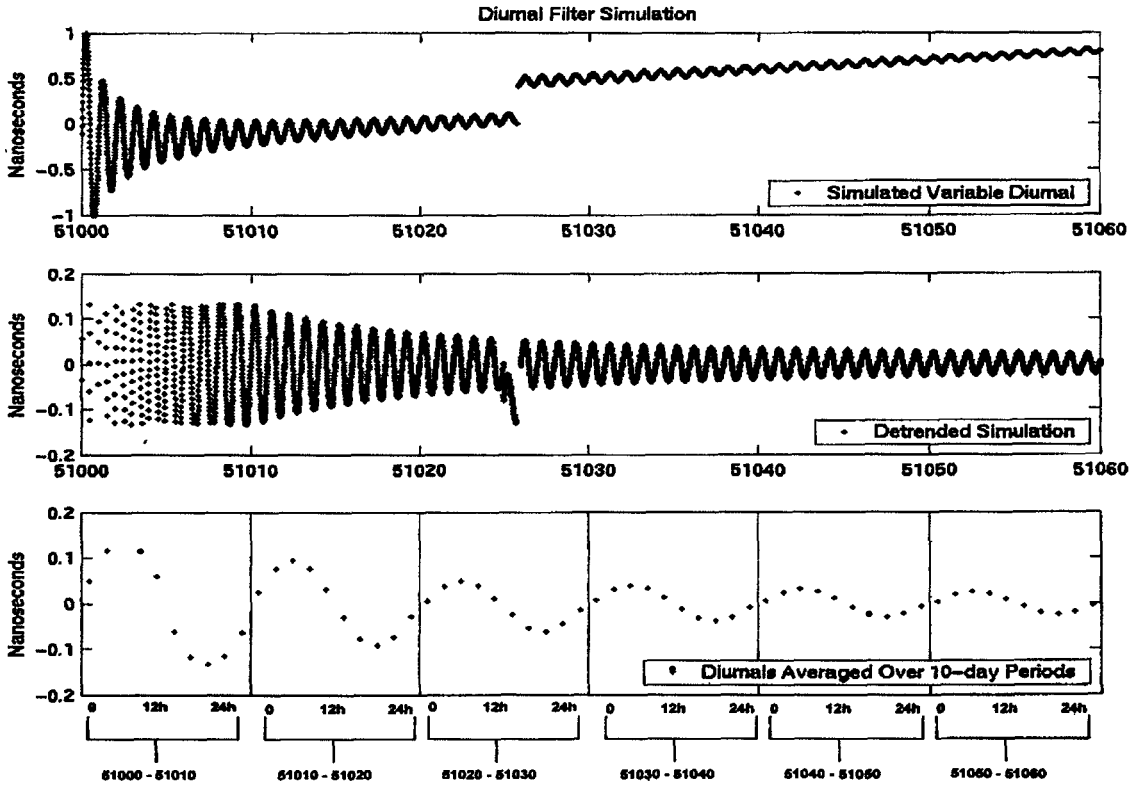

Figure 7. Upper plot shows a computer-generated test time series. Middle plot shows how that time series would appear once filtered. The lower plot shows the 10-day average binned diurnals plotted side by side. As shown in the next figure, the x-axis of the lower plot is really the time of day of each 10-day average, whose start-time is identified by the axis label.

An effort was made to infer the environmental sensitivity of the code data by a linear fit of code residuals to meteorological data, which are publicly available at *ftp://cddisa.gsfc.nasa.gov.* It was found that 50 days of data typically yielded formal errors of order 4 ps/deg C, 3 ps/% relative humidity, and 1 ps/mbar. Only upper limits were found for the relative humidity and pressure terms, and these were not considered further. In a code-only analysis using data from 8-14 July 2001, Kouba **[19]** noted a 1-3 hour lag between the temperature and code residuals at two Canadian sites (ALGO and DRAO); however, in this work the data were about as often fit better with lag=0.

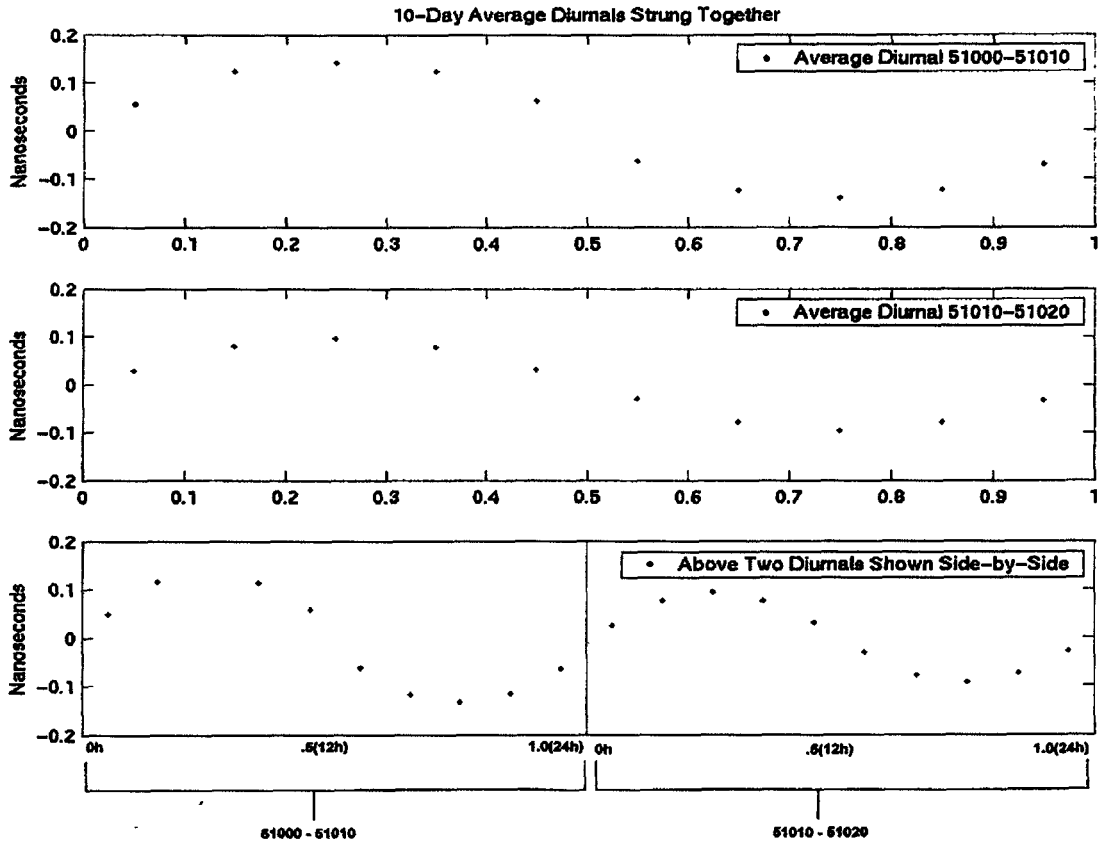

Figure 8. Illustration of how 10-day average binned diurnals are strung together. The top two plots show two different diurnals generated by averaging all filtered points corresponding to a given time of day over two adjacent 10-day periods. The x-axis is the fraction of a day. The lower plot shows the top two plots placed side by side. The lower plot of the previous figure is an extension of the process from two 10-day periods to many such.

In order to determine the appropriateness of the fitting to the residuals, independent linear fits of the code residuals to the exterior temperature were made for each day and site, from 13 July 2001-22 November 2001, and the fitted temperature dependencies are shown in Figures 13 and 14. The almost monotonic variations displayed by some sites and the irregularities displayed by other sites exceed what is expected from the formal errors to the daily fits. While it is beyond the scope of this work to determine what other factors are affecting the code residuals, these would be expected to include modifications in, or problems with, the GPS or meteorological hardware; nonlinearities in the temperature dependency of the hardware; changes in the location of, or temperature differentials between, the receiver, cabling, antenna, environ-

mental sensors and the exterior; and interference or multipath having a diurnal signature. It is clear that pseudorange variations are often dominated by error sources that mask simple temperature-related variations in the external equipment.

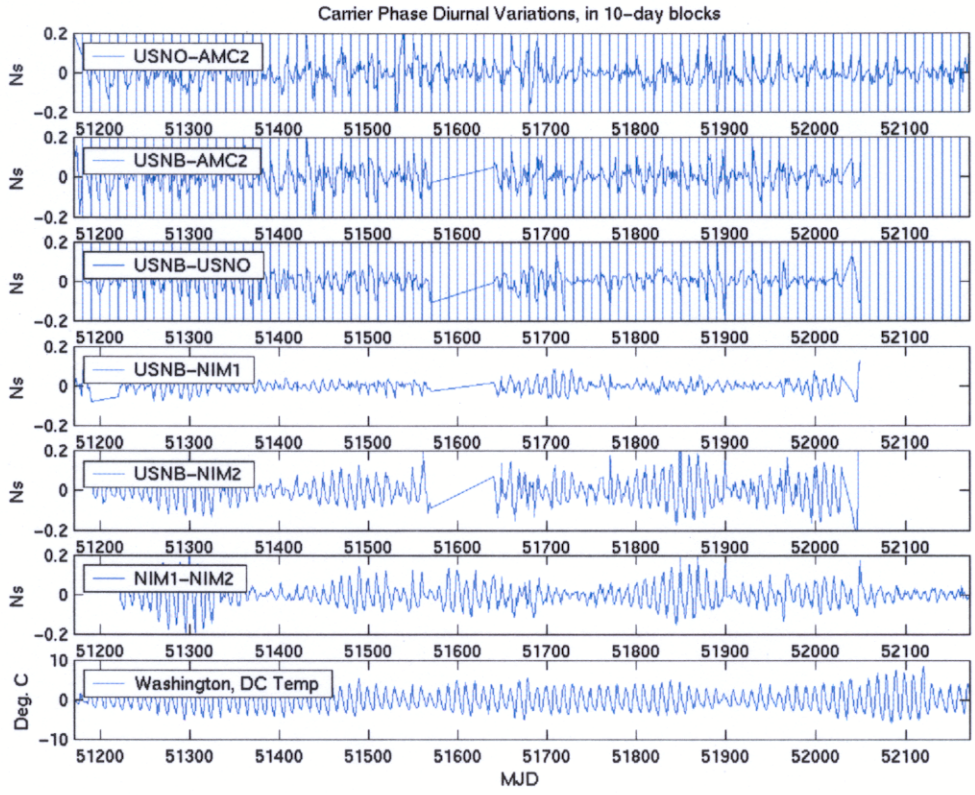

Figure 9. The diurnal signature in an average of 10 days of filtered and binned short-baseline data. The value plotted at MJD=10*N+m days is an average of all 24-hour filtered and hourly binned data between MJD=10*N and 10*N+10, where N= (MJD – MJD (modulo 10 days))/10, m is an integer between 0 and 9 inclusive (see formula in text), and MJD (modulo 1 day) $> 0.1*m$ and $< 0.1*(m+1)$. For example, the average diurnal from MJD 51220-51230 is plotted as if it were data from MJD 51220-51230; the difference between the points plotted at MJD 51225 and MJD 51220 is the difference between the data at UT=12 hours and UT=0 hours on MJD 51220 averaged with the same quantity on MJD 51221, 51222, …, 51229. Note that the diurnal was weaker in the winters (MJD 51550 was 7 January 2000), and fell dramatically when the GeTT (USNB) antenna cable was switched to a temperature-compensated cable on MJD 51714 (the cable type of the receiver USNO had been temperature-compensated all along). For clarity, only the upper plots show vertical lines denoting the separation between adjacent 10-day diurnals, which are labeled only by the start time of some of the bins. The Washington, DC temperature is treated in exactly the same manner for comparison purposes.

VIII. ANALYSIS NOISE AND OTHER ERROR SOURCES

TWSTT and CV data analyses consist mostly of simple data differencing that can be done within a PC and made available instantly. For CV, modeling the residual ionosphere and satellite orbit errors could

result in additional improvements for long baselines, at the 10-ns level **[17]**. For TWSTT, these error terms are not usually modeled and typically contribute about 100 ps, although the most extreme possibilities have been estimated to be 1 ns and 170 ps, respectively **[18]**.

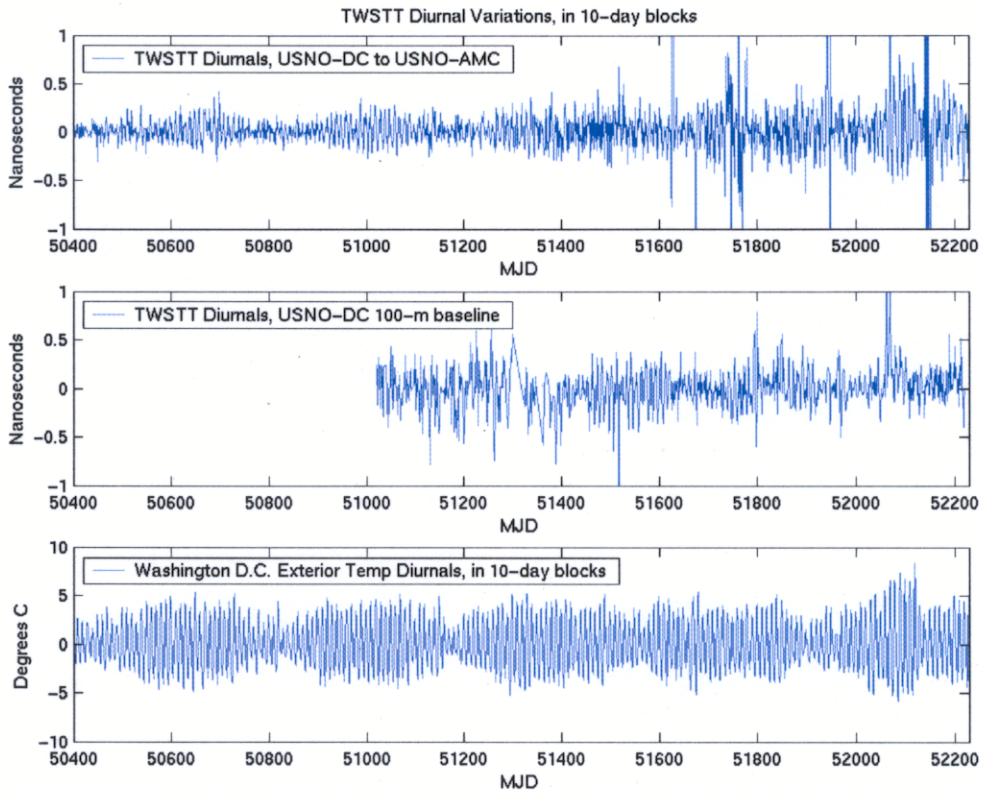

Figure 10. Diurnal variations in TWSTT data on continental and short baselines. Each sinusoid is the diurnal signature in an average of 10 days of filtered and binned data. The value plotted at MJD=10*N+m days is an average of all 24-hour filtered data between MJD=10*N and 10*N+10, where N= (MJD – MJD (modulo 10 days))/10, m is an integer between 0 and 9 inclusive (see formula in text), and MJD (modulo 1day) $> 0.1*m$ and $< 0.1*(m+1)$. For example, the average diurnal from MJD 51550-51560 is plotted as if it were data from MJD 51550-51560; the difference between the points plotted as MJD 51550 and MJD 51551 is the difference between the data at UT=2.4 hours and UT=0 hours on MJD 51550 averaged with the same difference on MJD 51551, 51552, …, 51559. As in previous figure, the x-axis label identifies the MJD of the start of each 10-day block, and the plotted points are an average of 10 MJDs at a given time of day.

It is well known that CP analysis is not severely impaired by orbital or atmospheric modeling errors, except perhaps at the day-boundary discontinuities. For example, based upon 5 days of CP data from 11 sites, we have found that changing the atmospheric mapping function from Lanyi to Neill changed no fitted (5-minute) clock parameter more than 10 ps and most less than 1 ps. Long-term (450-day) comparisons of inferred timing differences between about 30 pairs of sites reduced with IGS rapid orbit products instead of IGS final orbits show rms differences of 200-300 ps, except for pairs involving the USNO-DC antennas, which show an rms of about 100 ps. Presumably the entire difference is due to the lesser precision of the IGS rapid orbits. Continuously filtered CP data using IGS orbits that have 200 ps

discontinuities at day boundaries would be expected to display time discontinuities whose magnitude is much less due to projection effects, the ability to average over all satellites in view, and the insensitivity of the ambiguity parameters to the orbital correction.

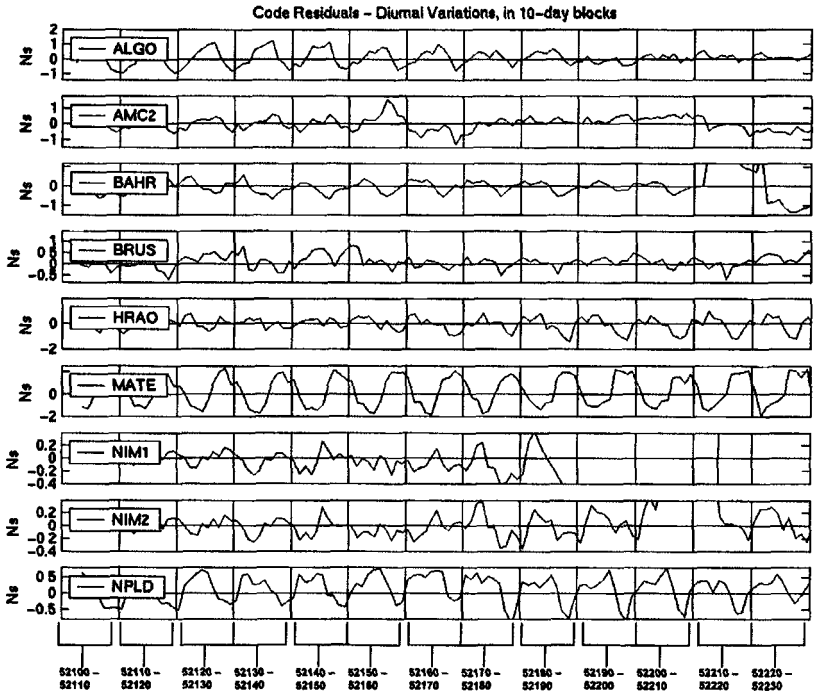

Figure 11. Diurnal signatures in code residuals of continuously filtered carrier-phase GPS solutions, for selected sites, from MJD 52100 through 52220, in 10-day bins. As illustrated in Figures 7 and 8, between each vertical line is a plot representing the average binned value for the 10-day period labeled on the x-axis. Points within the vertical bars represent the average diurnal for the 10-day period: points to the left side are just after UTC 0 hours, the point at the middle of each 10-day block is the average of 10 data taken at UTC 12 hours, and points to the right side approach UTC 24 hours. Formal errors are based upon the fit residuals.

One possible vulnerability of CP analysis is its mathematical complexity. For example, it has been observed that simply adding additional sites to the Kalman filter analysis of a small highly asymmetric array can change the time transfer at the 1-ns level **[20]**. However, we have seen that operational solutions by CODE and the USNO Associate IGS Analysis Center (run by the USNO Earth Orientation Department) do not display such frequency variations and their time-transfer solutions typically stay within 1 ns peak-to-peak, except for the few days on which the formal errors are high. The two centers use different software, different algorithms, and different sites in their analyses.

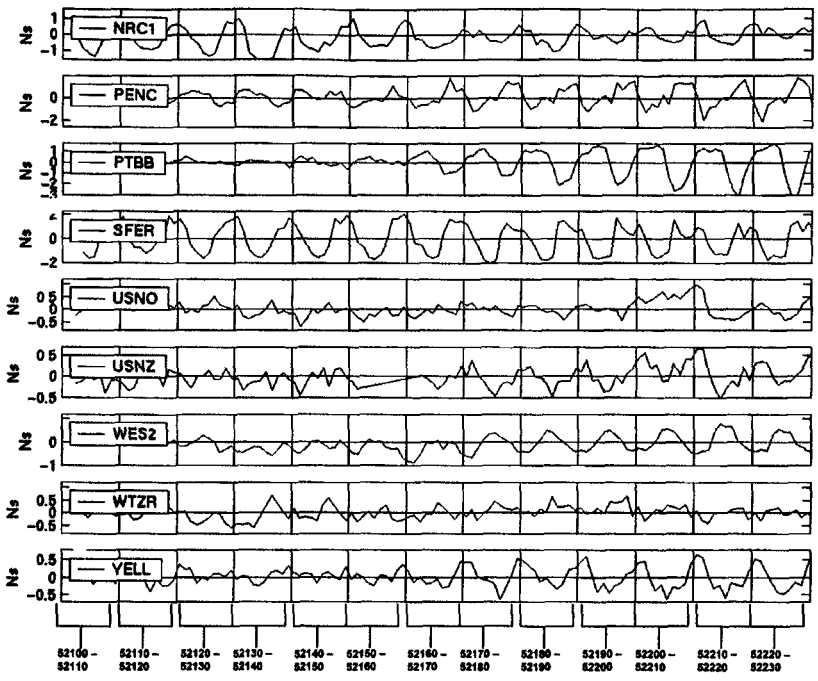

Figure 12. Continuation of previous figure. As illustrated in Figures 7 and 8, between each vertical line is a plot representing the average binned value for the 10-day period labeled on the x-axis. Points in the middle of each 10-day block are the average value at UTC 12 hours.

The day-boundary discontinuities in independent daily GPS carrier-phase time-transfer reductions may be due to starting time-transfer solutions anew at 00:00 hours UTC of each day **[4]**, with the resulting discontinuities displaying approximately 200-600 ps rms at the day boundaries. These jumps are assumed here to be due to the short (24-hour) time interval available to "average out" the noise in the pseudorange data, which are weighted so as to have a negligible effect on all parameters except the one to which phase data cannot contribute. This is the average time offset, which is equivalent to a constant of integration for the frequency. This implies that one could predict the observed day-boundary jumps between independent solutions from the daily average code residuals of continuously filtered solutions.

To test the idea that code residuals of continuously filtered solutions are related to the day-boundary jumps of independent daily solutions, independent daily solutions were generated over a 30-day period, and the day-boundary jumps predicted by the code residuals were subtracted. The rms day-boundary jumps of the corrected plots were significantly less, as shown in Table 2. Figure 15 shows a typical case. Although the large day-boundary jumps are removed, residual jumps remain; these may be due to immature parameters at the boundaries of the independent solutions, the finite smoothing of the continuous filter, or because the corrections derived from the residuals did not incorporate the effective error model used by GIPSY. Another contribution may be that the code residuals are sensitive to the difference between the code and phase temperature dependencies, whereas the day-boundary jumps are sensitive only to the code-temperature dependencies. The code-temperature dependencies are expected to exceed the phase-temperature dependencies in the electronics **[5,6]**, but variations in the cable delay would mitigate this by adding an equal amount of delay to both.

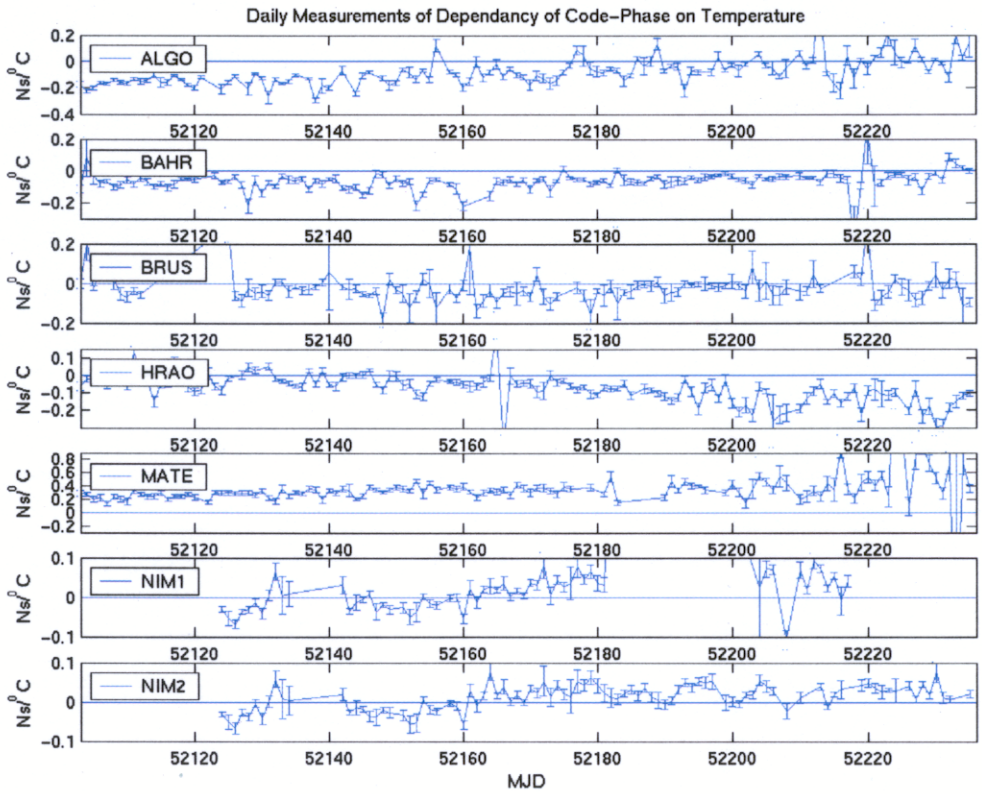

Figure 13. Fitted daily temperature dependencies of code residuals to continuously filtered solutions, for those sites in Figure 11 whose meteorological data were available at *ftp://cddisa.gsfc.nasa.gov* or measured at USNO. The formal errors of the computed temperature dependencies, determined by the scatter of the temperature-fit residuals, are consistent with the scatter of adjacent points. For ALGO, they are initially 10-20 ps/deg C, with an increasing number exceeding 50 towards MJD 52220. For BAHR, they are mostly 10-30 ps/deg C.

Comparisons of our continuously filtered solutions with independent 1-day solutions generated by CODE suggest that continuous filtering improves the short-term stability of GPS carrier-phase analysis (Figures 16-17), at least over the USNO's 150-m baseline. The possibility that this is due to the different networks and data reduction tools is unlikely because similar results are found in comparisons with independent daily solutions generated by the USNO's Earth Orientation department. Those comparisons cover only the period from December 1998 until March 1999, but the analysis tools and *a priori* assumptions were very similar to those used for the continuously filtered solutions reported here. Note that continuous filtering shows a smoother variation than the independent solutions during the period when the GeTT's (USNB's) temperature varied (beginning roughly MJD 51760, as described in Section II). This is because the sensitivity of the GeTT's phase data to temperature is less than the sensitivity of its code data **[7]**. The continuous filtering followed the phase data's variations in the short run, and gradually began to follow the code data. Since each 5-minute phase datum has a weight of about 10,000 times larger than its corresponding code datum, it would take about 30 days for the much larger error due to the phase fluctuations to be fully incorporated into the time-transfer solutions by the software. The observed smoothing is somewhat more rapid than this, but a more detailed analysis cannot be done because the actual temperature of the GeTT's receiver was not recorded.

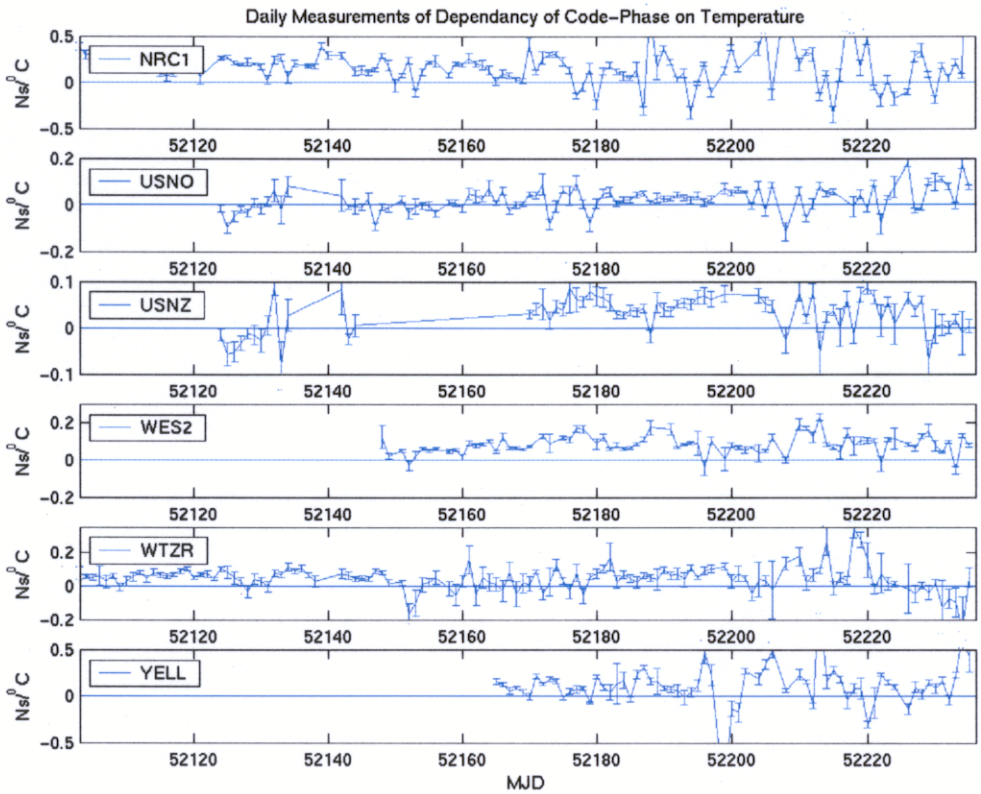

Figure 14. Daily temperature dependencies of code residuals, for those sites in Figure 12 whose meteorological data were available at *ftp://ccdisa.gsfc.nasa.gov* or measured at the USNO. The formal errors of the derived temperature dependencies are consistent with the observed scatter of adjacent points. For the USNO, they average 20 ps/deg C.

Comparisons of our continuously filtered solutions with independent 1-day solutions generated by CODE suggest that continuous filtering improves the short-term stability of GPS carrier-phase analysis (Figures 16-17), at least over the USNO's 150-m baseline. The possibility that this is due to the different networks and data reduction tools is unlikely because similar results are found in comparisons with independent daily solutions generated by the USNO's Earth Orientation department. Those comparisons cover only the period from December 1998 until March 1999, but the analysis tools and *a priori* assumptions were very similar to those used for the continuously filtered solutions reported here. Note that continuous filtering shows a smoother variation than the independent solutions during the period when the GeTT's (USNB's) temperature varied (beginning roughly MJD 51760, as described in Section II). This is because the sensitivity of the GeTT's phase data to temperature is less than the sensitivity of its code data **[7]**. The continuous filtering followed the phase data's variations in the short run, and gradually began to follow the code data. Since each 5-minute phase datum has a weight of about 10,000 times larger than its corresponding code datum, it would take about 30 days for the much larger error due to the phase fluctuations to be fully incorporated into the time-transfer solutions by the software. The observed smoothing is somewhat more rapid than this, but a more detailed analysis cannot be done because the actual temperature of the GeTT's receiver was not recorded.

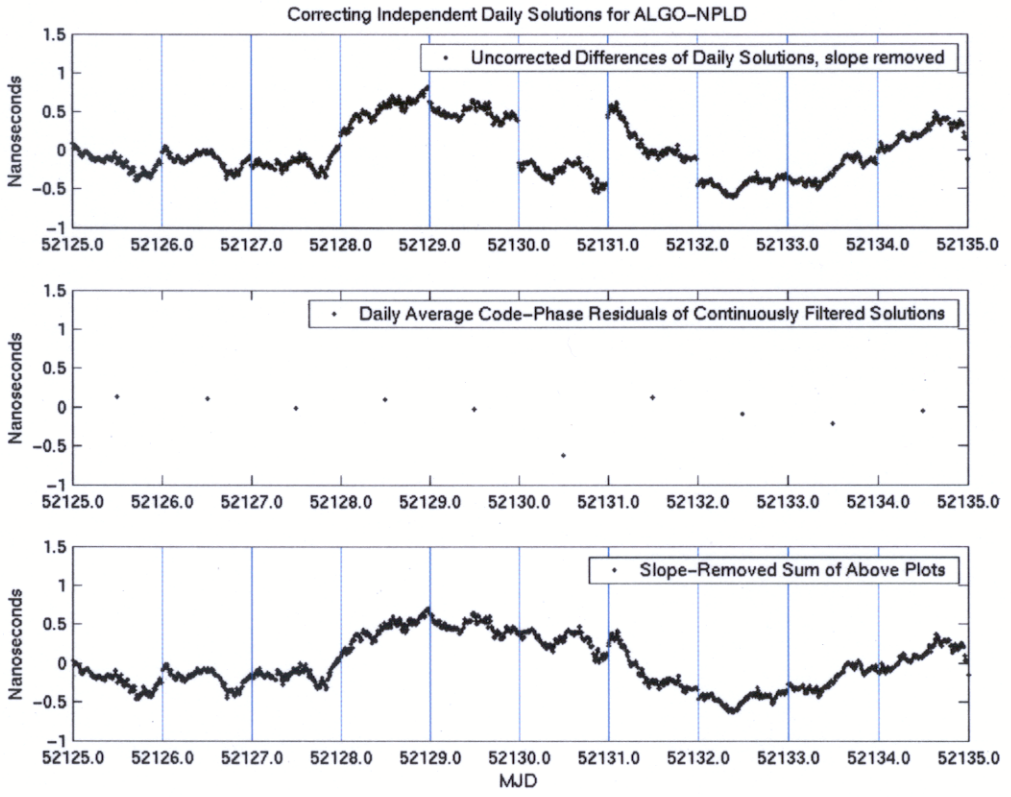

Figure 15. Day-boundary jumps observed with independent daily solutions, shown in the top plot, are largely removed by subtracting the unweighted daily average of the code residuals of continuously filtered solution, as shown in the bottom plot. The complete analysis is summarized in Table 2.

It has been shown that unmodelled site position errors, and presumably any incorrectly modelled parameter that is dependent on elevation or azimuth, could lead to a frequency error in continuous filtering situations **[21]**. However, site positions are solved for in typical time-transfer solutions, and the USNO's continuously filtered solutions have not been observed to deviate systematically from daily batch solutions (Figures 18 and 19). Since site parameter reinitialization occurs whenever data are missing or rejected, we conservatively conclude that continuous filtering, as practiced, remains the preferred technique, subject to any limitations due to computer resources or process timeliness. Should it be shown that systematic errors could accumulate through truly continuous filtering, one solution would be to apply modern control theory **[22]** to steer continuously filtered results to either the kinds of 1-day arc solutions currently generated by the IGS centers, or perhaps solutions continuously filtered over several-day arcs.

Table 2. Rms day-boundary discontinuities in ps, over 30 days, of independent daily solutions before and after correction by adding the average code residual of the corresponding continuously filtered solutions. The effects of orbital discontinuities and clock variations were minimized by subtracting continuously filtered clock differences from the independent daily results. ALGO was used as a reference, but the closure property limits the sensitivity to the reference somewhat. Sites with asterisk had highly variable timing solutions, for which the unmodelled weighting would lead to the largest errors in the correction. Note that continuously filtered clock differences typically have no discernable day-boundary jumps.

SITE	Uncorrected	Corrected
ALGO-AMC2	372	185
ALGO-BAHR	325	281
ALGO-BOR1	201	194
ALGO-GODE*	299	191
ALGO-GRAZ	376	223
ALGO-HRAO*	416	470
ALGO-KOKB*	378	360
ALGO-LPTF	517	352
ALGO-MDVO	433	337
ALGO-MKEA*	366	173
ALGO-NIM1	366	173
ALGO-NIM2	405	162
ALGO-NPLD	404	174
ALGO-NRC1	439	221
ALGO-NRC2	497	206
ALGO-NYA1*	467	251
ALGO-NYAL	442	268
ALGO-OBE2*	394	338
ALGO-PENC	411	255
ALGO-PIE1*	469	317
ALGO-PTBB	381	224
ALGO-SFER*	448	364
ALGO-USNO	336	192
ALGO-USNZ	380	170
ALGO-WES2*	321	156
ALGO-WTZR	429	240
ALGO-YELL	537	235

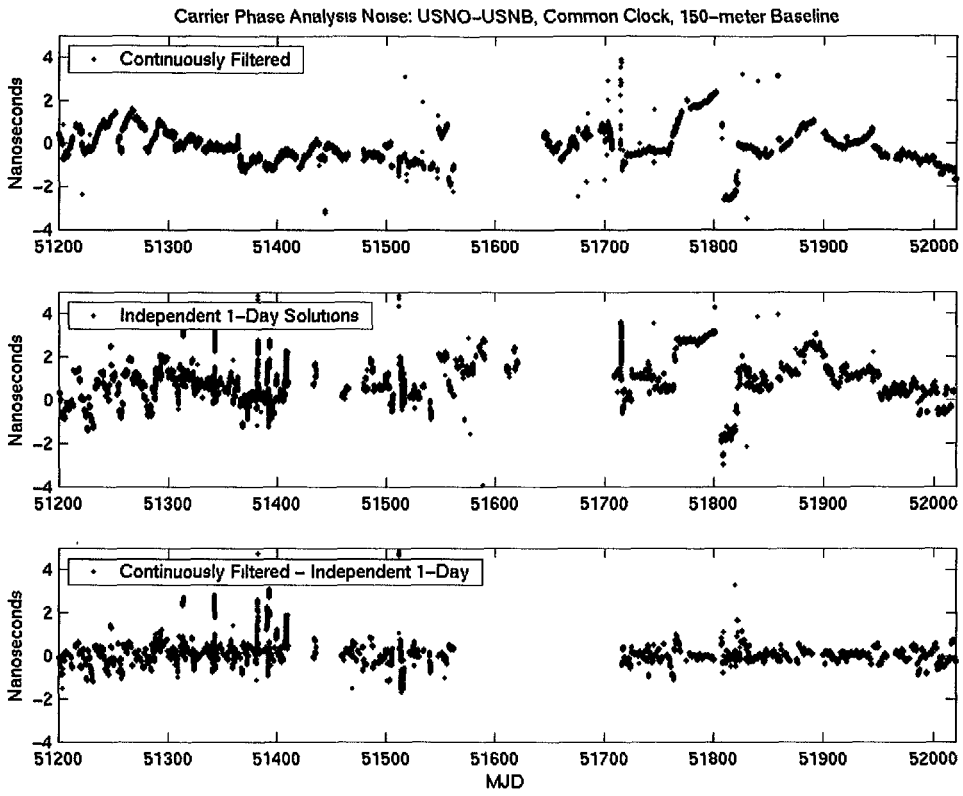

Figure 16. Top: USNO short-baseline data reduced using continuous filtering. Middle: same data reduced using independent solutions for each day, as reduced by CODE. The improvement in the short-term precision of CODE's independent 1-day solutions after MJD 51700 may be due to improved outlier removal. Bottom: Difference between upper two plots.

IX. CLOSURE AS A MEASURE OF TIME-TRANSFER STABILITY

CP analyses are completely site-based; hence, time-transfer data from any three clocks A, B, and C will satisfy the relation (A-B)+(B-C)+(C-A)=0 as a constraint in the analysis software of the computer program. For CV, closure would be automatic for observations of individual satellites using site-dependent corrections, but it is not guaranteed for averages in which all sites do not observe the same satellites at the same times. Figure 20 shows TWSTT closure experiments involving the USNO-DC, NIST (Colorado), and either NPL (England) or PTB (Germany). The USNO-NIST data were taken using a satellite different from the European links, yet the closure has been satisfied within the few-hundred ps limits of the short-term noise. A systematic difference of perhaps 100 ps before and after the data gap of MJD 50100-50500 is apparent in the USNO-NIST-PTB data, which could perhaps be due to satellite motion not having been accounted for in those observations.

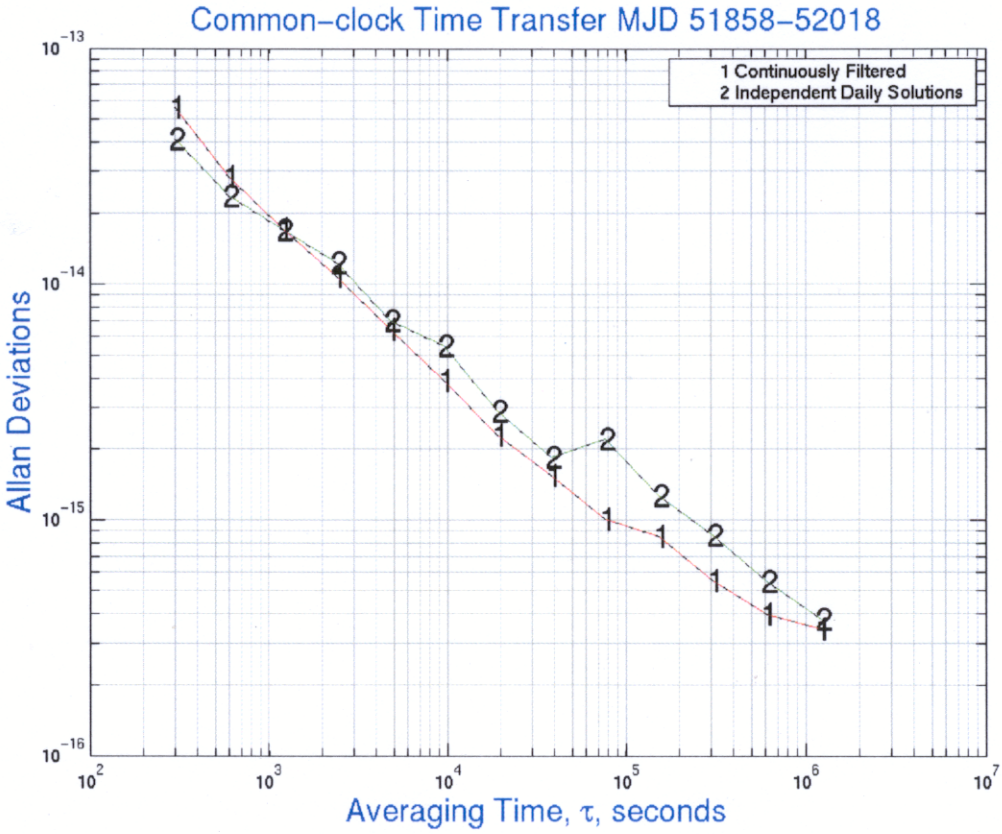

Figure 17. Allan deviations of short-baseline common-clock data of the previous figure, from MJD 51859 through MJD 52018. Continuously filtered solutions were produced by the authors; the independent day boundary solutions were produced by CODE, but are similar to those produced by the USNO Earth Orientation Department's independent daily solutions. Data were corrected to a common clock through use of hourly round-trip-corrected cable and fiber measurements whose basic one-way measurement precision is 20-50 ps. The lesser stability of the independent daily solutions at 1 day is a reflection of their day-boundary discontinuities. The inferred subdaily stabilities are increased by the precision of the hourly ground-based direct clock measurements, and the slope of the continuously filtered Allan deviations is observed to be -.61; the slope is -.77 for tau < 20,000 seconds.

IX. CONCLUSIONS

Direct comparisons of GPS common-view, GPS carrier-phase, and TWSTT time-transfer precisions over short and long distances have the potential to distinguish between the stability of different modes. GPS carrier-phase data show long-term maximum variations of up to 10 ns when compared to calibrated and recalibrated TWSTT, and the associated worst-case frequency drift is $< 6\ 10^{-16}$. Continuously filtered GPS carrier phase, which largely eliminates the day-boundary discontinuities of independent daily solutions, shows no apparent decrease in long-term precision. TWSTT and many of the GPS systems show diurnal signatures in their frequency-transfer results; studies of the GPS code residuals in continuously filtered solutions can reveal time-variable apparent instrumental temperature dependencies, which are relevant to time transfer. None of the systems have yet been truly optimized and all are being improved in many ways.

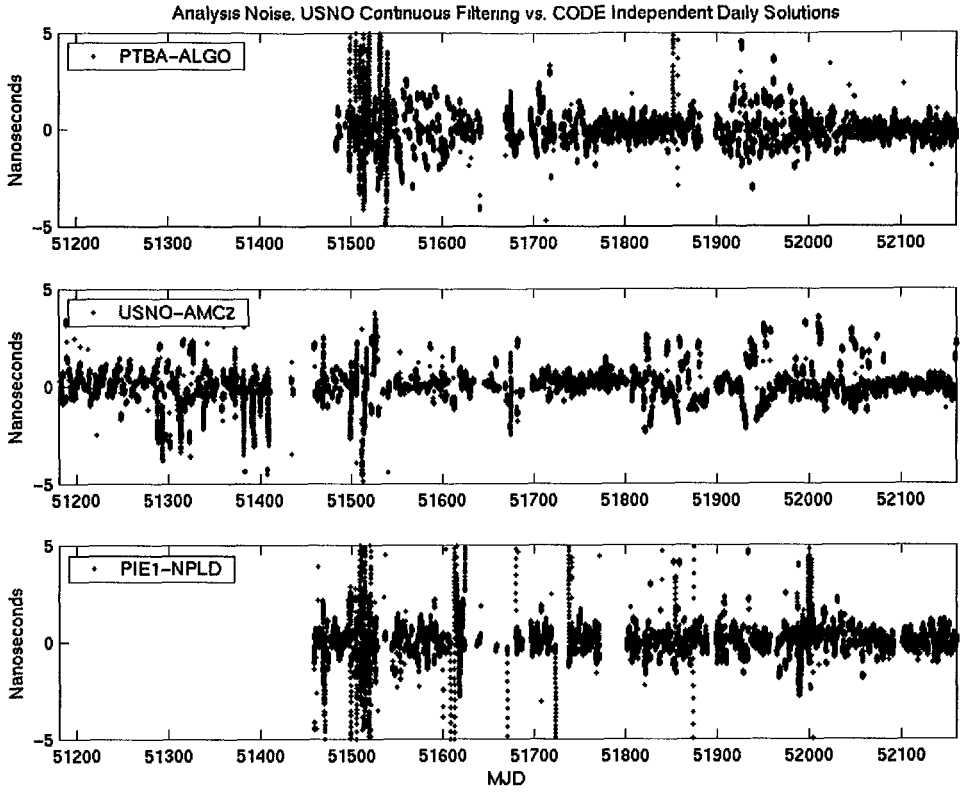

Figure 18. Difference between continuously filtered carrier phase solutions, by the authors, and solutions generated in independent 1-day batches by CODE, for continental and transatlantic baselines. The locations of the receivers PTBA and NPLD are at the PTB (Germany) and NPL (England), while PIE1 and AMC2 are in the western United States.

X. DISCLAIMER

The USNO cannot endorse any commercial product. We caution the reader that the equipment quality described here may not be characteristic of similar equipment maintained at other laboratories, nor of equipment currently marketed by any commercial vendor.

XII. ACKNOWLEDGMENTS

We thank the staff of Network Control Center Geospacial Science Center, NIMA St. Louis for allowing the use of the data from their receivers, and we thank Rolf Dach and Tom Schildknecht of the University of Berne, Switzerland, and Gregor Dudle and Leon Prost of the Swiss Federal Office of Metrology for the use of the GeTT data. We thank the USNO staff, particularly Ed Powers, Kenneth Johnston, and Dennis McCarthy, for many helpful discussions.

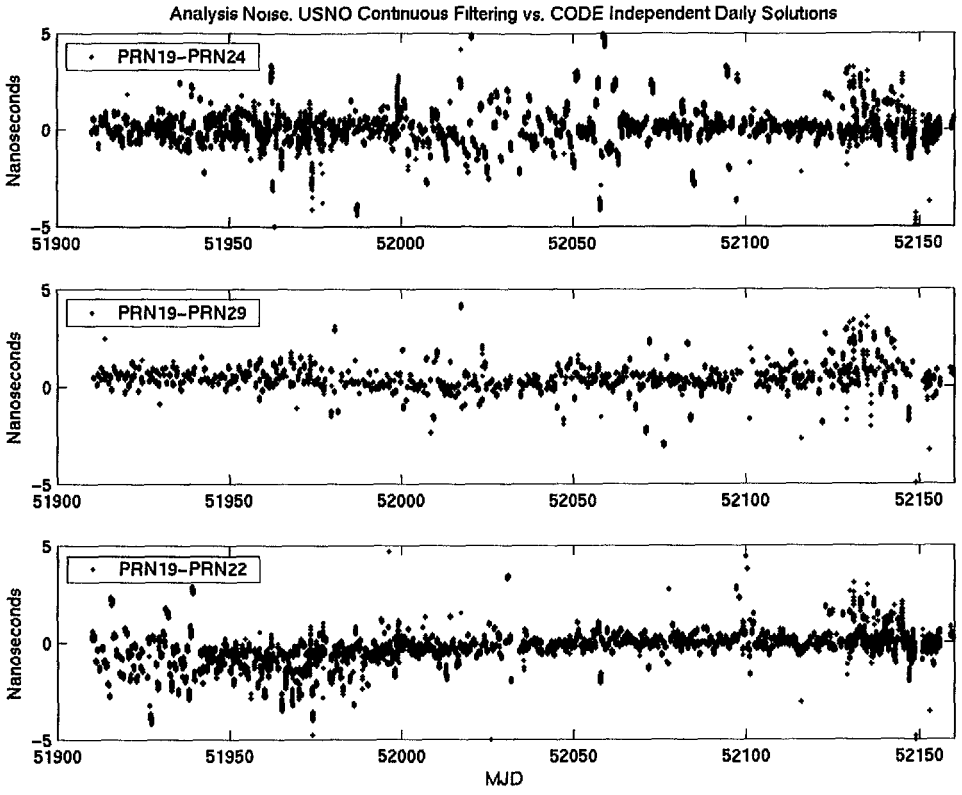

Figure 19. Difference between continuously filtered carrier-phase solutions, by the authors, and solutions generated in independent 1-day batches by CODE, for the timing difference between two GPS satellites.

XIV. REFERENCES

[1] D. Allan and C. Thomas, 1994, *"Technical Directives for Standardization of GPS Time Receiver Software,"* **Metrologia, 31,** 69-79.

[2] D. N. Matsakis, L. Schmidt, K. Senior, E. Powers, and J. DeYoung, 2001, *"Comparison of High-Precision Time Transfer Techniques,"* in Proceedings of the International Conference on Time and Frequency, 6-7 February 2001, New Delhi, India, pp. 115-132.

[3] A. Schaefer, A. Pawlitzki, and T. Kuhn, 2000, *"New Trends in Two-Way Time and Frequency Transfer via Satellite,"* in Proceedings of the 31st Annual Precise Time and Time Interval (PTTI) Systems and Applications Meeting, 7-9 December 1999, Dana Point, California, USA, pp. 505-514.

[4] K. Senior, E. Powers, and D. Matsakis, 2000, *"Attenuating Day-Boundary Discontinuities in GPS Carrier Phase Time-Transfer,"* in Proceedings of the 31st Annual Precise Time and Time Interval (PTTI) Systems and Applications Meeting, 7-9 December 1999, Dana Point, California, USA, pp. 481-490.

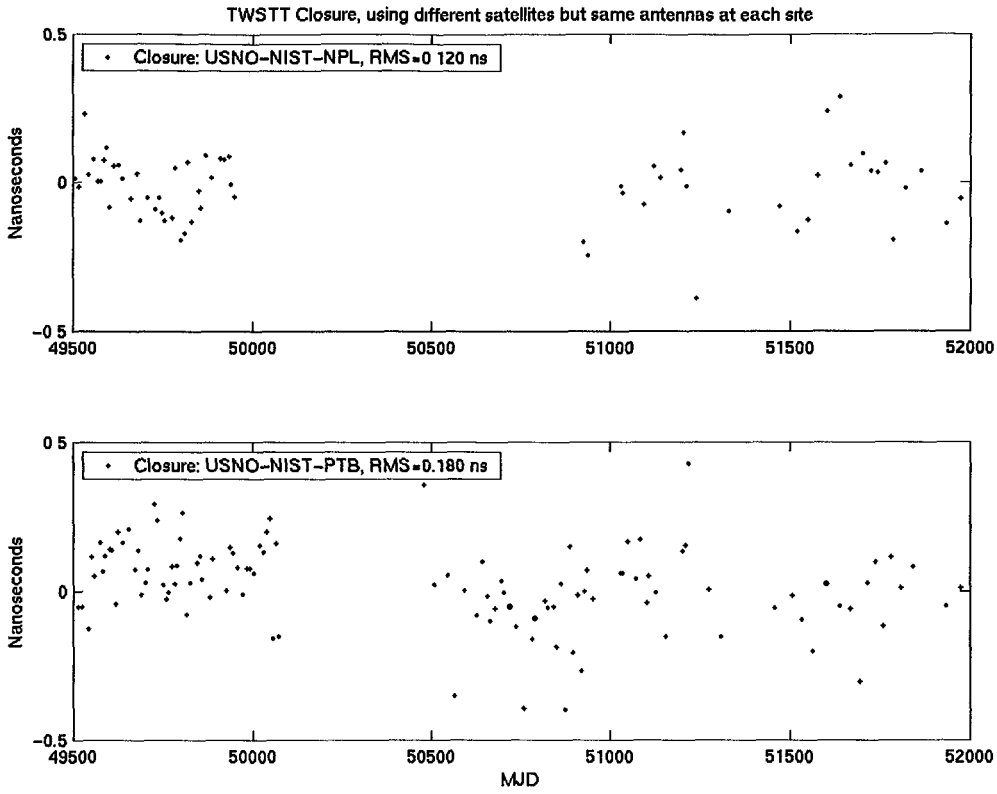

Figure 20. Closure on USNO/NIST/NPL and USNO/NIST/PTB baselines. Data taken as part of the BIPM's time-transfer program, which does not directly measure the USNO-NIST time differences, are combined with an independent series of observations between USNO and NIST.

[5] E. Powers, 1999, *"Hardware Measurements and Sensitivities in Carrier Phase Time Transfer,"* in Proceedings of the 30th Annual Precise Time and Time Interval (PTTI) Systems and Applications Meeting, 1-3 December 1998, Reston, Virginia, USA, pp. 307-314.

[6] E. Powers, 2000, *"Calibration of GPS Time Transfer Equipment,"* in Proceedings of the 31st Annual Precise Time and Time Interval (PTTI) Systems and Applications Meeting, 7-9 December 1999, Dana Point, California, USA, pp. 441-448.

[7] F. Overney, L. Prost, U. Feller, T. Schildknecht, and G. Beutler, 1997, *"GPS Time Transfer using Geodetic Receivers: Middle Term Stability and Temperature Dependence of Signal Delays,"* in Proceedings of the 11th European Frequency and Time Forum (EFTF), 4-7 March 1997, Neuchâtel, Switzerland, pp. 504-508.

[8] R. Dach, T. Schildknecht, and T. Springer, 2001, *"A Transatlantic GeTT Time Transfer Experiment – Latest Results,"* in Proceedings of the 32nd Annual Precise Time and Time Interval (PTTI) Systems and Applications Meeting, 28-30 November 2000, Reston, Virginia, USA, pp. 67-77.

[9] E. Powers, 2001, private communication.

[10] Robert Snow, private communication.

[11] E. Powers, K. Senior, Y. Bar-Server, W. Bertiger, R. Muellerschoen, and D. Stowers, 2002, *"Real Time Ultra-Precise Time Transfer to UTC Using the NASA Differential GPS System,"* in these Proceedings.

[12] B. Tolman, and D. Munton, 2002, *"GPS Carrier Phase Frequency Transfer On the NIMA Monitor Station Network,"* in these Proceedings.

[13] D. Matsakis, K. Senior, and E. Powers, 2000, *"Analysis Noise, Short-Baseline Time Transfer, and a Long-Baseline Carrier Phase Frequency Scale,"* in Proceedings of the 31st Annual Precise Time and Time Interval (PTTI) Systems and Applications Meeting, 7-9 December 1999, Dana Point, California, USA, pp. 491-504.

[14] K. Larson and J. Levine, 1999, *"Carrier-Phase Time Transfer,"* **IEEE Transactions on Ultrasonics, Ferroelectrics, and Frequency Control, UFFC-46,** 1001-1012.

[15] J. Ray and K. Senior, 2001, *"Temperature Sensitivity of the Dorne Morgolin Antennas,"* **GPS Solutions, 5**(1), 24-30.

[16] F. Ascarrunz, T. Parker, and S. Jefferts, 1999, *"Pseudo-random Code Correlator Timing Errors Due to Multiple Reflections in Transmission Lines,"* in Proceedings of the 30th Annual Precise Time and Time Interval (PTTI) Systems and Applications Meeting, 1-3 December 1998, Reston, Virginia, USA, pp. 433-438.

[17] L. Schmidt and R. Kramer, 1999, *"Effects of Ionosphere Delay on GPS Time Transfer,"* in Proceedings of the 12th International Technical Meeting of the Satellite Division of the Institute of Navigation, ION-GPS, 14-17 September 1999, Nashville, Tennessee, USA (ION, Alexandria, Virginia), pp. 1073-1079.

[18] D. Kirchner, 1999, *"Two Way Satellite Time and Frequency Transfer (TWSTFT),"* **Review of Radio Science** (Oxford Science Publications, Oxford, UK), pp. 27-44.

[19] J. Kouba, 2001, *"Investigation of the Daily Periodical Errors of GPS.C Pseudorange Clock Solutions,"* unpublished.

[20] L. Nelson and J. Levine, 2001, *"Examining GPS Carrier-phase Analysis to Evaluate the Accuracy of Frequency Transfer Using Data from NIST and PTB,"* in Proceedings of the 32nd Annual Precise Time and Time Interval (PTTI) Systems and Applications Meeting, 28-30 November 2000, Reston, Virginia, USA, pp. 57-66.

[21] R. Dach, 2000, presentation at IGS/BIPM Working Group meeting, U.S. Naval Observatory, Washington, D.C., USA.

[22] P. Koppang and R. Leland, 1999 *"Linear Quadratic Stochastic Control of Atomic Hydrogen Masers,"* **IEEE Transactions on Ultrasonics, Ferroelectronics, and Frequency Control, UFFC-46,** 517-522.